Identification of Bistability in Enzymatic Reaction Networks Using Hysteresis Response

Takashi Naka*
Faculty of Science and Engineering, Kyushu Sangyo University, Fukuoka, Japan

Keywords: Enzymatic Reaction Network, Regulatory Network, Hysteresis Response, Bistability, Mathematical Model.

Abstract: Intracellular signaling systems can be viewed as enzymatic reaction networks in which enzymes regulate each other through activation and inactivation, and exhibit various properties such as bistability depending on their regulatory structure and parameter values. In this study, we formulate the intracellular signaling systems as regulatory networks whose nodes are cyclic reaction systems of enzyme activation and inactivation, and propose an evaluation function that can identify bistability with low computational cost. For the purpose of demonstrating its effectiveness, we identified 4- and 5-node regulatory networks that exhibit bistability. Furthermore, the effect of parameter values on bistability was analyzed, suggesting that the regulatory structure is more dominant than parameter values for the emergence of bistability.

1 INTRODUCTION

Intracellular signaling systems can be viewed as enzymatic reaction networks in which enzymes regulate each other through activation and inactivation, and are known to exhibit various characteristics depending on their regulatory relationships and parameter values (Ferrell, 1998; Jeschke et al., 2013; Kholodenko, 2006; Mai & Liu, 2013; Qiao et al., 2007; Volinsky & Kholodenko, 2013). For example, the MAPK cascade, one of the most representative and well analyzed enzymatic reaction network, has been reported to have ultrasensitive properties that can function as an analog-to-digital conversion in the cell. It has also been shown that it can be bistable as an extreme case.

Multistability, represented by bistability, corresponds to a stable group of states in the cell and is thought to provide robust control over intra- and extracellular disturbances (Gedeon et al., 2018; Ma et al., 2009; Yao et al., 2011). Bistability is also an important property from the standpoint of synthetic biology, as it may function as a memory element (Doncic et al., 2015). Therefore, it is interesting to know what kind of regulatory structures and parameter values of enzymatic reaction networks show bistability, and studies have been conducted to analyze the properties of enzymatic reaction networks by changing the structure and parameter values of the networks in an exhaustive manner (Kuwahara & Gao, 2013; Ramakrishnan & Bhalla, 2008; Shah & Sarkar, 2011; Siegal-Gaskins et al., 2011; Sueyoshi & Naka, 2017).

In order to identify enzymatic reaction networks with specific properties, such as bistability, an evaluation function is needed to quantify the degree of the property. It is also necessary to select an appropriate mathematical model to describe the enzymatic reaction networks. With respect to the number of enzyme species that comprise the enzymatic reaction network, several efforts have been made to address the combinatorial increase in computational cost of their identification.

One innovation is the simplification of the mathematical model of enzymatic reactions. Enzymatic reactions can be described by a system of differential equations by applying the law of mass action, but to reduce computational cost, the Michaelis-Menten or linear approximation is sometimes used (Adler et al., 2017; Kuwahara & Gao, 2013; Ma et al., 2009; Shah & Sarkar, 2011; Sueyoshi & Naka, 2017; Yao et al., 2011). However, if possible, the analysis would be more accurate without those approximations. In fact, with respect to bistability, it has been suggested that the Michaelis-Menten approximation overstates the evaluation

* http://www.is.kyusan-u.ac.jp/~naka/

Naka, T.
Identification of Bistability in Enzymatic Reaction Networks Using Hysteresis Response.
DOI: 10.5220/0012416000003657

In *Proceedings of the 17th International Joint Conference on Biomedical Engineering Systems and Technologies (BIOSTEC 2024) - Volume 1*, pages 479-486
ISBN: 978-989-758-688-0; ISSN: 2184-4305

(Kim & Tyson, 2020; Naka, 2020). Therefore, in this study, we use a mathematical model that does not make any approximations, only applying the law of mass action.

There are also several methods for the evaluation function of bistability. An enzymatic reaction network has two kinds of parameters: the total concentration of each enzyme that makes it up and the reaction rate constants for each enzyme. For a particular set of parameter values of a system, there are possible ways to transition from a random initial value group to a steady state (Naka, 2022). If the system is bistable and a sufficient number of initial value groups are used, bistability can be detected due to the system transitions to two values of steady states. However, the computational cost is higher because steady-state values must be obtained for a number of initial value groups.

Another possible method is to fix one value of a certain reaction rate constant, etc. as an input to the system, and then gradually change the value to obtain a steady state sequentially. If the system is bistable, it takes advantage of the property that different steady-state values are reached when its input values are increased or decreased. This is less computationally expensive than the aforementioned method. This method will be referred to as the sequential steady-state tracking method in this study. Figure 1 shows an example of a regulatory network consisting of 4 nodes. In this study, we propose an evaluation function using hysteresis response that extends the sequential steady-state tracking method and verify its effectiveness.

The MAPK cascade, a representative signaling system that relays between the plasma membrane and cell nucleus with respect to cell growth factor (EGF) signaling, is thought to be the cause of cell cancer, and much has been learned about its abnormalities (Ferrell, 1998; Jeschke et al., 2013; Kholodenko, 2006; Mai & Liu, 2013; Qiao et al., 2007; Volinsky & Kholodenko, 2013). A major component of the signaling system represented by the MAPK cascade is the enzymatic activation/inactivation cyclic reaction system through phosphorylation and dephosphorylation of enzymes. The cyclic reaction system is a combination of two post-translational modification reactions. Therefore, we model and analyze the intracelluler signaling system as a regulatory network consisting of enzymatic activation/inactivation cyclic reaction systems, which mutually regulate each other.

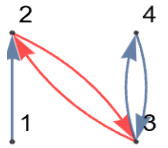

Figure 1: Regulatory network consisting of 4 nodes. The number is the node number. Node 1 is an input node. Node 4 is the output node. Blue and red arrows represent positive and negative regulations, respectively.

2 REGULATORY NETWORKS TO BE ANALYZED

The regulatory network is a representation of the regulatory relationships between enzymes, where each node included corresponds to a cyclic reaction system of enzymatic activation and inactivation. The cyclic reaction system is an enzymatic reaction system that combines two post-translational modification reactions represented by phosphorylation. It is represented by the following reaction scheme.

$$\mathrm{U_i} + \mathrm{S_i} \underset{d_i}{\overset{a_i}{\rightleftharpoons}} \mathrm{Q_i} \xrightarrow{k_i} \mathrm{P_i} + \mathrm{S_i}$$

$$\mathrm{P_i} + \mathrm{V_i} \underset{e_i}{\overset{b_i}{\rightleftharpoons}} \mathrm{R_i} \xrightarrow{l_i} \mathrm{U_i} + \mathrm{V_i}$$

$\mathrm{U_i}$ is the inactive form of the enzyme, $\mathrm{S_i}$ is the activating enzyme that catalyzes the activation of $\mathrm{U_i}$, $\mathrm{Q_i}$ is the enzyme-substrate complex to which $\mathrm{U_i}$ and $\mathrm{S_i}$ are bound, $\mathrm{P_i}$ is the active form of the enzyme, $\mathrm{V_i}$ is the inactivating enzyme that catalyzes the inactivation of $\mathrm{P_i}$, $\mathrm{R_i}$ is the enzyme-substrate complex to which $\mathrm{P_i}$ and $\mathrm{V_i}$ are bound. a_i, d_i, k_i, b_i, e_i, and l_i are the reaction rate constants for each reaction. The subscript i is the node number in the regulatory network.

By applying the law of mass action to the reaction scheme, we obtain a system of differential equations describing the behavior of the system shown below.

$$\alpha_i = a_i U_i S_i - d_i Q_i,\ \beta_i = k_i Q_i$$

$$\gamma_i = b_i P_i V_i - e_i R_i,\ \delta_i = l_i R_i$$

$$\frac{\mathrm{d}U_i}{\mathrm{d}t} = -\alpha_i + \delta_i,\ \frac{\mathrm{d}S_i}{\mathrm{d}t} = -\alpha_i + \beta_i,\ \frac{\mathrm{d}Q_i}{\mathrm{d}t} = \alpha_i - \beta_i$$

$$\frac{\mathrm{d}P_i}{\mathrm{d}t} = \beta_i - \gamma_i,\ \frac{\mathrm{d}V_i}{\mathrm{d}t} = -\gamma_i + \delta_i,\ \frac{\mathrm{d}R_i}{\mathrm{d}t} = \gamma_i - \delta_i$$

The activated enzyme $\mathrm{P_i}$ catalyzes the activation or inactivation reaction of the enzyme at the other node.

Figure 1 shows an example of a regulatory network consisting of 4 nodes. The blue arc from node *j* to node *i* means that the activated enzyme P_j at node *j* is catalyzing the activation reaction of the enzyme at node *i* as the activated enzyme S_i. This is called node *j* positively regulating node *i*. The red arc from node *j* to node *i* means that the activated enzyme P_j at node *j* is catalyzing the inactivation reaction of the enzyme at node *i* as the inactivating enzyme V_i. This is called node *j* negatively regulating node *i*.

In this study, assuming a typical signaling system such as a MAPK cascade, we will analyze regulatory networks with 4 and 5 nodes that satisfy the following constraints.

- It has one input node and one output node, and is connected from the input node to the output node with positive or negative regulations through intermediate nodes.
- Each node receives at most two regulations, positive and negative, from the other nodes.
- Each node regulates at most two other nodes.
- There is no auto-regulaton.
- The input node is node 1 and is not regulated by any other node.
- The output node is node *N* if the number of nodes is *N*. Since a regulation of the outside of the regulatory network is assumed for the output node, the output node regulates at most one other node in the regulatory network.

There are 80 regulatory networks of 4 nodes and 912 regulatory networks of 5 nodes that satisfy the above conditions.

3 IDENTIFICATION OF BISTABILITY USING THE HYSTERESIS RESPONSE

The value of the reaction rate constant k_1 of the cyclic reaction system corresponding to the input node is the external input to the regulatory network, which is the oscillatory stimulus in the following equation.

$$k_1(t) = \frac{\sin\left(\frac{2\pi}{T}\left(t - \frac{T}{4}\right)\right) + 1}{2}$$

T is the period of oscillation. In this study, the period was set to 3600 seconds, i.e. 1 hour. This is large enough to allow time for the intracellular signaling system to reach a steady state.The system is intended to maintain an approximate steady state in its response to the oscillatory input. The output of the regulatory network is the relative concentration P_N of the activated enzyme at node *N* if the number of nodes is *N*.

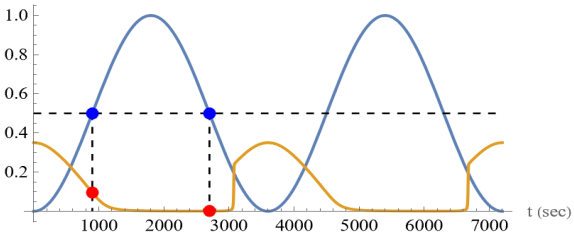

Figure 2: Oscillatory input and the response. Response of the output enzyme activity to the oscillatory input stimulus for the regulatory network of Fig. 1. The blue curve is the time course of k_1, the input to the system. Two periods are displayed. The ochre curve is the time course of the relative concentration of P_4, the output of the system. The red circle corresponds to the value of the output when the value of the input is 0.5, indicated by the blue circle.

Figure 2 shows an example of the response of the 4-node regulatory network shown in Fig. 1 to a oscillatory input. The total concentration of each enzyme and the reaction rate constant are all set to 1, except for k_1, the input to be varied. The unit system is the μM-sec system. The blue curve is the time course of k_1, the input to the system. Two periods are displayed. The ochre curve is the time course of the relative concentration of P_4, the output of the system. The time course of the output differs when the input is increasing and when it is decreasing, indicating the appearance of hysteresis. When the input is increasing, the output gradually decreases as the input increases, but when the input is decreasing, the output is almost zero until the value of the input is around 0.25, at which point it rapidly increases. The red circle in the figure corresponds to the value of the output when the input value is 0.5, indicated by the blue circle. It can be seen that the values are different when the input is increasing and when it is decreasing.

The phase diagram between input k_1 and output P_4 in Fig. 2 is shown in Fig. 3. The blue and red circles correspond to those in Fig. 2. The upper right-descending line corresponds to the output when the input is rising, and the lower curve corresponds to the output when the input is decreasing. It can be seen that a typical hysteresis appears, where the response differs between rising and falling inputs. From the figure, it can be read that the input is bistable in the range of 0.2 to around 0.8.

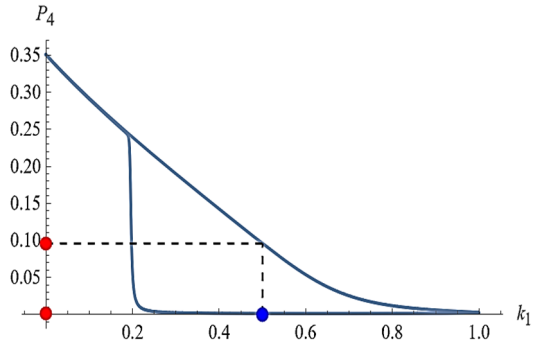

Figure 3: Hysteresis on the oscillatory response. Phase diagram of the input k_1 and output P_4 in Fig. 2. The blue and red circles correspond to those in Fig. 2.

The hysteresis loss H is used as a quantitative measure of the bistability of the system, which is formulated as bellow.

The hysteresis loss is the area of the closed region appearing in the phase diagram. The area is approximated by a finite sum of T/d time intervals, where T is the period of the input and d is the number of divisions. Since both input and output are normalized to a maximum value of 1, the maximum hysteresis loss is 1. In this study, the value of the number of divisions d is set to 50. The convergence rate C is used to quantify the degree of convergence of the hysteresis loss, which is formulated as bellow. This is the difference between the hysteresis loss in the first period and the hysteresis loss in the subsequent period.

Figure 4 shows the hysteresis loss using the sequential steady-state tracking method mentioned above. This is a method in which the steady-state

$$H = \sum_{i=0}^{d/2-1} \left| k_1(t_{i+1}) - k_1(t_i) \right| \times \left| P_4(t_i) - P_4(T - t_i) \right|, \quad t_i = \frac{T}{d} i$$

value of the system is first obtained with zero input, and the value at that time is used as the initial value, and the steady-state value is obtained sequentially as the input is gradually increased. Therefore, the accuracy is considered to be higher than the method using hysteresis response proposed here. However, if this method is executed in a form corresponding to the number of divisions mentioned above, a convergence calculation of the system is performed for the number of divisions, and the computational

$$C = \frac{\sum_{i=0}^{d-1} \left| k_1(t_{i+1}) - k_1(t_i) \right| \times \left| P_4(t_i) - P_4(t_i + T) \right|}{2}, \quad t_i = \frac{T}{d} i$$

cost is at least the number of division times. The curves in Fig. 4 is similar to that in Fig. 3 using hysteresis, indicating that the hysteresis-based method proposed here is effective. Mathematica

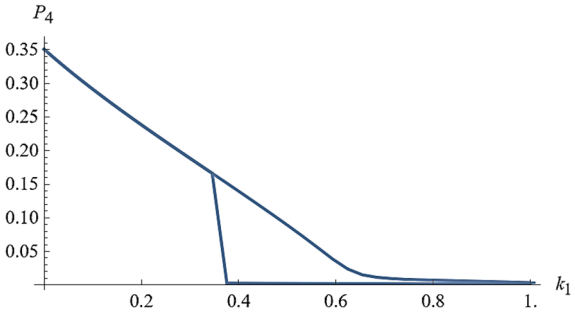

Figure 4: Hysteresis on the steady state. Hysteresis loss by sequential steady-state tracking method.

v13.0 was used to derive a system of differential equations describing the behavior of the system from the enzymatic reaction network and to numerically solve the derived system of differential equations to calculate hysteresis loss H and convergence rate C, and to analyze bistability (Wolfram Research, 2021).

4 IDENTIFICATION OF BISTABLE REGULATORY NETWORKS

The results of the analysis for 80 regulatory networks of 4 nodes that satisfy the constraints are shown in Fig. 5. The horizontal axis is the hysteresis loss H and the vertical axis is the convergence rate C. The total concentration of each enzyme and the reaction rate constants, all set to 1, are circled in red. The unit system is μM-sec.

To further investigate the effect of reaction rate constants on hysteresis loss, the reaction rate constants of the nodes other than the input node were varied. However, to prevent the combination of parameters from becoming too large, the six values included in the cyclic reaction system comprising each node were kept the same value. The range of change was set to 11 values of 2^p (p is an integer from -5 to 5) to approximately include the values used in the literature as reaction rate constants for the enzymes comprising the MAPK cascade (Brightman & Fell, 2000; Hatakeyama et al., 2003; Huang & Ferrell, 1996; Levchenko et al., 2000; Schoeberl et al., 2002). On the other hand, with respect to the input node, k_1 among the reaction rate constants of that cyclic reaction system was assumed to be the oscillatory input and all other reaction rate constants were fixed at 1, since it is intended to change the concentration of P_1, which is the input to node 2. Thus, the total number of combinations of parameters is 11^3=1331. In practice, however, the values of all

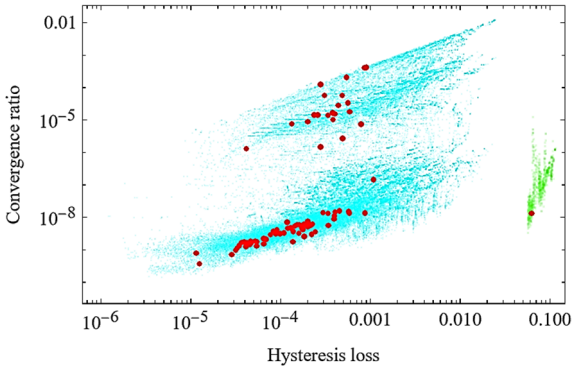

Figure 5: Aspect of hysteresis on 4 nodes networks. Results for 80 4-node regulatory networks. The horizontal axis is the hysteresis loss H and the vertical axis is the convergence rate C. The red circles are the results when the total concentration of each enzyme and the reaction rate constants are all set to 1. The other set of fine dots correspond to the case where the reaction rate constants of the nodes other than the input node are varied.

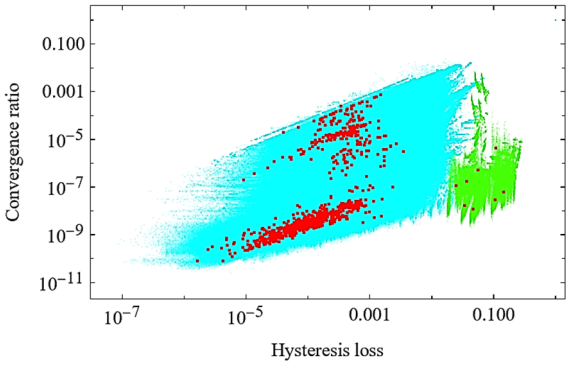

Figure 6: Aspect of hysteresis on 5 nodes networks. Results for 912 5-node regulatory networks. The horizontal axis is the hysteresis loss H and the vertical axis is the convergence rate C. The red circles are the results when the total concentration of each enzyme and the reaction rate constants are all set to 1. The other set of fine dots correspond to the case where the reaction rate constants of the nodes other than the input node are varied.

reaction rate constants are multiplied by a factor of 10 for the purpose of increasing the rate of convergence. This is the same as multiplying the period of the oscillatory input by a factor of 10, which means that the velocity of the oscillation is slowed down to 1/10.

The results are shown as a set of blue and green fine dots in Fig. 5. Only one regulatory network had a hysteresis loss value of about 0.1. The hysteresis loss of 0.1 is a fairly prominent value for the hysteresis loss region in the phase diagram. This regulatory network corresponds to the red circle and the fine green points isolated on the right side of the figure. This is the regulatory network used as an example in Fig. 1 through Fig. 4. Compared to the distribution of the red circles, the variation due to the parameter values indicated by the fine colored dots is distributed over a limited small area. This suggests that the network structure is dominant with respect to the property of bistability and robust with respect to parameter values, despite the limitation that the reaction rate constants within each node are identical.

There are 912 regulatory networks of 5 nodes that satisfy the constraints. Figure 6 shows the results of the analysis. As in Fig. 5, the horizontal axis is the hysteresis loss H and the vertical axis is the convergence rate C.

The meaning of the red circles and colored fine point groups is the same as in Fig. 5. In the 6-node regulatory network, eight had hysteresis loss values greater than 0.01. These correspond to the eight red circles and green fine dots scattered on the right side of the fig. 6. As in the 5-node regulatory network, the variation due to the values of the parameters indicated by the fine blue and green dots is distributed in a limited area, compared to the distribution of the red circles. This suggests again that the network structure is dominant with respect to the bistability property and robust with respect to the parameter values, although there is still the restriction that the reaction rate constants within each node are identical.

Figure 7 shows 5-node regulatory networks with hysteresis loss greater than 0.01. The regulatory structure of the network and the phase diagram of input k_1 and output P_5 are laid out. It can be seen that the regulatory structure of the 4-node regulatory network, which exhibits the bistability shown in Fig. 1, is contained in the third from the top of the left column and the second from the top of the right column. It is a structure of mutual negative regulation between node 2 and node 3 and positive regulation between node 3 and node 4. The regulatory structures of the remaining three regulatory networks are also found to have similar structures, although there is intervening positive regulation in between.

5 CONCLUSIONS

For 4- and 5-node regulatory networks, where the cyclic reaction system is the node and the regulatory relationship between them is the arc, the method using hysteresis response for identifying bistability was found to be effective. This method has errors compared to the sequential steady-state tracking method, but the computational cost is much lower.

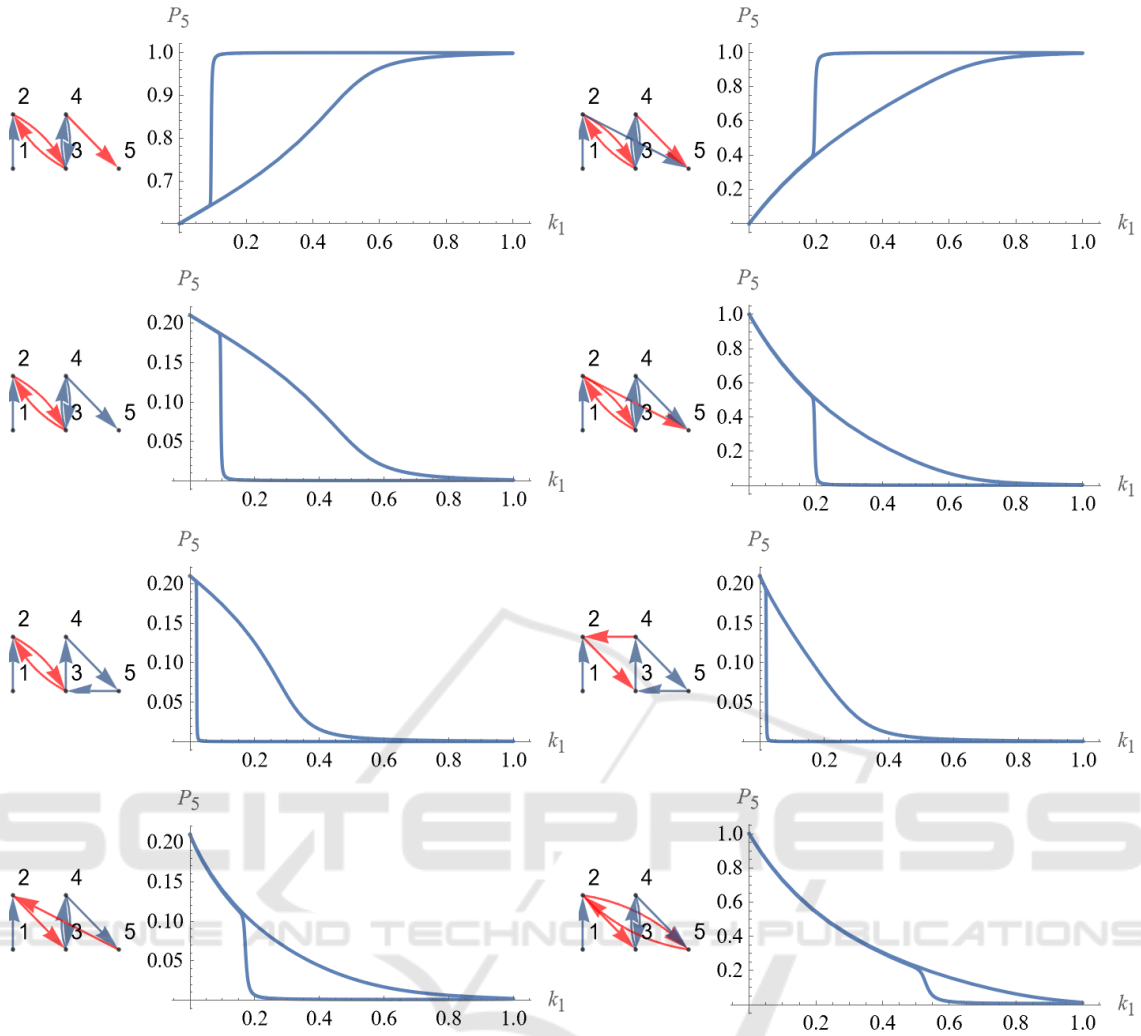

Figure 7: Bistable regulatory 5 nodes networks. 5-node regulatory networks with hysteresis loss greater than 0.01. The regulatory structure of the network and the phase diagram of input k_1 and output P_5 are laid out.

This error is not particularly problematic when it comes to primary screening of the regulatory networks.

The authors have proposed a representation of enzymatic reaction networks using set partitioning and a search algorithm based on the representation, in which a method with random initial value group is used as the evaluation function for bistability (Naka, 2022). The computational cost was therefore enormous, requiring time on the order of several days to complete the search. The evaluation function using hysteresis response proposed here is expected to have an application to search as well, since its cost is expected to be about 1/100 of that estimated from its computational complexity. In fact, most of the computational cost is the convergence calculation performed to find the steady state of the system. In the sequential steady state tracking method used to validate the proposed method, the convergence calculation must be performed as many times as the number of divisions of the parameter values to be analyzed, which in this study is set at 50, resulting in a computational cost approximately 50 times higher. Furthermore, the method using a random initial value group described above requires a sufficient number of initial values to separate two transition destinations in a bistable system. Even if the value is set to about 10, the convergence calculation must be performed about 500 times, i.e., the number of initial values multiplied by the number of divisions. In the evaluation function using the hysteresis response proposed here, the convergence calculation to find the steady state of the system only needs to be performed once to find the

initial values, and as a result, the computational cost is about 1/100 of the original cost.

The results also suggest that the regulatory structure of the network is dominant with respect to the bistability compared to the parameter values. This indicates that, when searching for regulatory networks with bistability, it may be effective, for example, to fix all parameter values to 1 and search for variations in structure only.

By the way, the enzymatic reaction networks analyzed here were cyclic reaction systems as nodes. The MAPK cascade, a typical signal transduction system, includes the process of double phosphorylation. To extend the mathematical model of this study to include the process of double phosphorylation in the analysis, the set of differential equations derived from a single node can be modified. In the future, we intend to extend it as such and apply it to a more realistic analysis of bistability in intracellular signaling systems.

REFERENCES

Adler, M., Szekely, P., Mayo, A., & Alon, U. (2017). Optimal Regulatory Circuit Topologies for Fold-Change Detection. *Cell Syst*, *4*(2), 171-181 e178. https://doi.org/S2405-4712(16)30419-7 [pii], 10.1016/j.cels.2016.12.009

Brightman, F. A., & Fell, D. A. (2000). Differential feedback regulation of the MAPK cascade underlies the quantitative differences in EGF and NGF signalling in PC12 cells. *FEBS Letters*, *482*, 169-174.

Doncic, A., Atay, O., Valk, E., Grande, A., Bush, A., Vasen, G., Colman-Lerner, A., Loog, M., & Skotheim, J. M. (2015). Compartmentalization of a bistable switch enables memory to cross a feedback-driven transition. *Cell*, *160*(6), 1182-1195. https://doi.org/10.1016/j.cell.2015.02.032, S0092-8674(15)00198-1 [pii]

Ferrell, J. E., Jr. (1998). How regulated protein translocation can produce switch-like responses. *Trends in Biochemical Science*, *23*, 461-465.

Gedeon, T., Cummins, B., Harker, S., & Mischaikow, K. (2018). Identifying robust hysteresis in networks. *PLoS Comput Biol*, *14*(4), e1006121. https://doi.org/10.1371/journal.pcbi.1006121 PCOMPBIOL-D-17-01583 [pii]

Hatakeyama, M., Kimura, S., Naka, T., Kawasaki, T., Yumoto, N., Ichikawa, M., Kim, J. H., Saito, K., Saeki, M., Shirouzu, M., Yokoyama, S., & Konagaya, A. (2003). A computational model on the modulation of mitogen-activated protein kinase (MAPK) and Akt pathways in heregulin-induced ErbB signalling. *Biochemical Journal*, *373*(Pt 2), 451-463.

Huang, C. F., & Ferrell, J. E., Jr. (1996). Ultrasensitivity in the mitogen-activated protein kinase cascade. *Proceedings of the National Academy of Science of the United States of America*, *93*, 10078-10083.

Jeschke, M., Baumgartner, S., & Legewie, S. (2013). Determinants of cell-to-cell variability in protein kinase signaling. *PLoS Comput Biol*, *9*(12), e1003357. https://doi.org/10.1371/journal.pcbi.1003357 PCOMPBIOL-D-13-00825 [pii]

Kholodenko, B. N. (2006). Cell-signalling dynamics in time and space. *Nat Rev Mol Cell Biol*, *7*(3), 165-176. http://www.ncbi.nlm.nih.gov/entrez/query.fcgi?cmd=Retrieve&db=PubMed&dopt=Citation&list_uids=16482094

Kim, J. K., & Tyson, J. J. (2020). Misuse of the Michaelis-Menten rate law for protein interaction networks and its remedy. *PLoS Comput Biol*, *16*(10), e1008258. https://doi.org/10.1371/journal.pc bi.1008258

Kuwahara, H., & Gao, X. (2013). Stochastic effects as a force to increase the complexity of signaling networks. *Sci Rep*, *3*, 2297. https://doi.org/10.1038/srep02297 srep02297 [pii]

Levchenko, A., Bruck, J., & Sternberg, P. W. (2000). Scaffold proteins may biphasically affect the levels of mitogen-activated protein kinase signaling and reduce its threshold properties. *Proceedings of the National Academy of Science of the United States of America*, *97*(11), 5818-5823.

Ma, W., Trusina, A., El-Samad, H., Lim, W. A., & Tang, C. (2009). Defining network topologies that can achieve biochemical adaptation. *Cell*, *138*(4), 760-773. https://doi.org/10.1016/j.cell.2009.06.013 S0092-8674(09)00712-0 [pii]

Mai, Z., & Liu, H. (2013). Random parameter sampling of a generic three-tier MAPK cascade model reveals major factors affecting its versatile dynamics. *PLoS One*, *8*(1), e54441. https://doi.org/10.1371/journal.pone.0054441 PONE-D-12-24261 [pii]

Naka, T. (2020). Validity of the Michaelis-Menten Approximation for the Stability Analysis in Regulatory Reaction Networks. BIOSTEC 2020 (13th International Joint Conference on Biomedical Engineering Systems and Technologies), Valletta, Malta.

Naka, T. (2022). The partition representation of enzymatic reaction networks and its application for searching bi-stable reaction systems. *PLoS One*, *17*(1), e0263111. https://doi.org/10.1371/journal.pone.0263111

Qiao, L., Nachbar, R. B., Kevrekidis, I. G., & Shvartsman, S. Y. (2007). Bistability and oscillations in the Huang-Ferrell model of MAPK signaling. *PLoS Comput Biol*, *3*(9), 1819-1826. https://doi.org/07-PLCB-RA-0294 [pii] 10.1371/journal.pcbi.0030184

Ramakrishnan, N., & Bhalla, U. S. (2008). Memory switches in chemical reaction space. *PLoS Comput Biol*, *4*(7), e1000122. https://doi.org/10.1371/journal.pcbi.1000122

Schoeberl, B., Eichler-Jonsson, C., Gilles, E. D., & Muller, G. (2002). Computational modeling of the dynamics of the MAP kinase cascade activated by surface and internalized EGF receptors. *Nature Biotechnology*, *20*, 370-375.

Shah, N. A., & Sarkar, C. A. (2011). Robust network topologies for generating switch-like cellular responses. *PLoS Comput Biol*, *7*(6), e1002085.

https://doi.org/10.1371/journal.pcbi.1002085 10-PLCB-RA-2608 [pii]

Siegal-Gaskins, D., Mejia-Guerra, M. K., Smith, G. D., & Grotewold, E. (2011). Emergence of switch-like behavior in a large family of simple biochemical networks. *PLoS Comput Biol*, *7*(5), e1002039. https://doi.org/10.1371/journal.pcbi.1002039 PCOMPBIOL-D-10-00298 [pii]

Sueyoshi, C., & Naka, T. (2017). Stability Analysis for the Cellular Signaling Systems Composed of Two Phosphorylation-Dephosphorylation Cyclic Reactions. *Computational Molecular Bioscience*, *7*, 33-45.

Volinsky, N., & Kholodenko, B. N. (2013). Complexity of receptor tyrosine kinase signal processing. *Cold Spring Harb Perspect Biol*, *5*(8), a009043. https://doi.org/10.1101/cshperspect.a009043a009043 [pii] 5/8/a009043 [pii]

Wolfram Research, I. (2021). *Mathematica*. In (Version 13.0)

Yao, G., Tan, C., West, M., Nevins, J. R., & You, L. (2011). Origin of bistability underlying mammalian cell cycle entry. *Mol Syst Biol*, *7*, 485. https://doi.org/10.1038/msb.2011.19msb201119 [pii]